ACS APPLIED MATERIALS & INTERFACES

Research Article

www.acsami.org

Polyhedral Oligomeric Silsesquioxane Functionalized Carbon Dots for Cell Imaging

Wen-Jing Wang,[†] Xin Hai,[†] Quan-Xing Mao,[†] Ming-Li Chen,*[,†] and Jian-Hua Wang*[,†,‡]

[†]Research Center for Analytical Sciences, Northeastern University, Box 332, Shenyang 110819, China

[‡]Collaborative Innovation Center of Chemical Science and Engineering, Tianjin 300071, China

Supporting Information

ABSTRACT: In the present study, octa-aminopropyl polyhedral oligomeric silsesquioxane hydrochloride salt (OA-POSS) functionalized carbon dots (CDs/POSS) are prepared by a one-pot approach with glycerol as carbon source and solvent medium. OA-POSS serves as a passivation agent, and it is obtained via hydrolytic condensation of 3-aminopropyltriethoxysilane (APTES). During the functionalization process, the amino groups on OA-POSS combine with carboxylic groups on the bare CDs via formation of amide bond to construct organic−inorganic hybrid carbon dots. The obtained CDs/POSS are well dispersed in aqueous medium with a diameter of ca. 3.6 nm. It is demonstrated that CDs/POSS provide favorable photoluminescent property with a quantum yield of 24.0%. They also exhibit resistance to photobleaching and excellent photoluminescence stability in the presence of biological sample matrix (characterized by heavy metals and organic molecules), which facilitate cell imaging in biological systems. Both the photoluminescent emission wavelength and the fluorescence intensity depend closely on the excitation wavelength, and thus, it provides a potential for multicolor imaging as demonstrated with HeLa cells and MCF-7 cells.

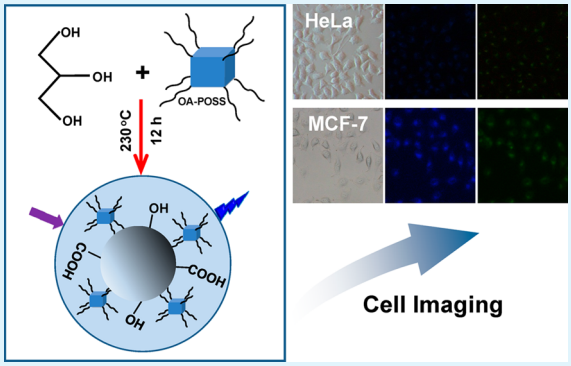

KEYWORDS: *polyhedral oligomeric silsesquioxane, functionalization, organic−inorganic hybrid, carbon dots, cell imaging*

INTRODUCTION

Carbon dots (CDs) as new emerging fluorescent carbon nanoparticles and rising stars of fluorescent quantum dots have gained tremendous attention in applications for bioimaging,[1−3] sensing of metal cations and biological molecules,[4−6] drug delivery,[3] white light emitting diodes,[7] and photo catalysis.[8] Generally, the preparation of CDs involves two approaches, namely, top-down and bottom-up,[9] among which a series of procedures or methods have been exploited, such as acid oxidation,[3,10] laser ablation,[11] electrochemical synthesis,[12] pyrolysis or carbonization of organic precursors[5,13] and preparations on solid supports.[14,15] In the preparation process, the choice of various carbon sources result in different characteristics for the obtained carbon dots. So far, a lot of carbon sources have been employed, including large-scale carbon material (e.g., carbon nanotubes,[12] candle soot,[10] and activated carbon[16]), natural materials[2,17−21] (e.g., cocoon silk,[2] banana juice,[17] orange juice,[18] food waste derived sources,[19] milk,[20] and bee pollens[21]), organic molecules (e.g., glycerol,[22] citric acid,[5] carbohydrates[23]), and polymers (e.g., polyethylenimine,[13] poly(ethylene glycol)[24]). However, bare carbon dots without surface functionalization or passivation generally exhibit very weak emissions in aqueous medium and other solvents.[25] The presence of abundant carboxyl groups or hydroxyl groups on the surface of carbon dots make it suitable for surface functionalization, passivation, or both with organic moieties or polymers.[26,27] This has been widely recognized as an effective approach for improving the quantum yield of CDs. Meanwhile, there is another method for this purpose, that is, doping[28] and codoping[29] with boron, nitrogen, sulfur, silicon, or phosphorus. Surface passivation or doping endows carbon dots with strong emission in the visible region, or even extending into the near-IR.[25]

As an organic−inorganic hybrid nanomaterial, polyhedral oligomeric silsesquioxane (POSS; $R_8Si_8O_{12}$) has an inorganic cubic-cage core which is ca. 0.53 nm in diameter. The eight organic arms can be easily functionalized with a wide variety of organic pendant groups such as $-NH_2$, $-SH$, $-OH$, and $-COOH$, which tend to provide abundant reactive sites for further functionalization. It is known that POSS has excellent biocompatibility and thermal and mechanical stability. It has been applied as antithrombogenic agent,[30] drug carrier,[31] and mesoporous organic−inorganic hybrid material.[32] It is worth mentioning that POSS has been used as ligand to produce photoluminescent nanoparticles, for example, water-soluble hybrid nanodots based on POSS and conjugated with oligoelectrolyte for two-photon excited fluorescence imaging of cellular nucleus,[33] CdSe quantum dots capped by SH-POSS as efficient photosensitizers for TiO_2 nanotube arrays,[34] lanthanide/europium β-diketonate complex functionalized

Received: May 14, 2015
Accepted: July 14, 2015
Published: July 14, 2015

DOI: 10.1021/acsami.5b04172
ACS Appl. Mater. Interfaces 2015, 7, 16609−16616

POSS with good thermal stability and luminescence properties,[35,36] Mn-doped ZnS quantum dots capped by OA-POSS and 3-mercaptopropionic acid for detecting DNA,[37] and near-infrared-emitting CdSeTe quantum dots fabricated with OA-POSS as the capping agent for SiHa cell imaging.[38] However, so far, POSS has never been reported as ligand for the construction of photoluminescent carbon dots.

As mentioned above, POSS can potentially interact with various functional groups, including carboxyl (−COOH) and hydroxyl (−OH), on the surface of bare CDs. In this study, octa-aminopropyl polyhedral oligomeric silsesquioxane hydrochloride salt (OA-POSS) is used as passivation agent for one pot preparation and functionalization of carbon dots (CDs/POSS) with glycerol as carbon source and solvent medium. The obtained CDs/POSS exhibit a high quantum yield and favorable photoluminescent property in addition to the characteristic features of carbon dots. CDs/POSS has proven to be suitable for cell imaging and shows great potential in biological applications.

EXPERIMENTAL SECTION

Materials and Reagents. Glycerol, hydrochloric acid, sulfuric acid, methanol, and dimethyl sulfoxide (DMSO) are obtained from Sinopharm Chemical Reagent Co. (Shanghai, China). Quinine sulfate and 3-aminopropyltriethoxysilane (APTES) are purchased from Aladdin Industrial Co. (Shanghai, China). 3-(4,5-Dimethylthiazol-2-yl)-2,5-diphenyltetrazolium bromide (MTT) assay kit is acquired from KeyGEN Biotech Co. (Nanjing, China). DMEM high glucose medium, fetal bovine serum, penicillin, streptomycin and 0.25% trypsin-EDTA are achieved from Hyclone (Thermo Fisher Scientific, Waltham, MA). All the chemicals are used as received without further purification. Deionized water of 18 MΩ cm is used throughout the experiments.

Instrumentation. The fluorescence spectra are recorded on F-7000 fluorescence spectrophotometer (Hitachi, Japan). The quantum yield of CDs/POSS is derived by measurement on a Fluoromax 4 fluorescence spectrometer (Horiba Scientific, France). UV−vis absorption spectra are obtained on a U-3900 UV−vis spectrophotometer (Hitachi, Japan). FT-IR spectra are obtained by a Nicolet-6700 FT-IR spectrophotometer (Thermo Fisher Scientific, Waltham, MA) within a range of 400−4000 cm^{-1}. Transmission electron microscopy (TEM) images are recorded on JEM-2100 (HR) transmission electron microscopy (JEOL, Japan). Thermogravimetric analysis (TGA) is carried out on a HCT-2 thermogravimetric analyzer (Beijing HengJiu Instruments, China) under nitrogen protection at a flowing rate of 20 mL min^{-1} and a heating rate of 10 °C min^{-1} within the range of 25−800 °C. XPS analysis is performed on an ESCALAB 250 surface analysis system (Thermo Electron, England). Nuclear magnetic resonance (NMR) spectroscopy including ^{1}H NMR, ^{13}C NMR, and ^{29}Si NMR spectra are recorded on an Avance II NMR spectrometer (Bruker, Switzerland) at 600 MHz using BBO probe with DMSO-d_6 as deuterated solvent and tetramethylsilane as the internal reference. Fluorescent microscope images of HeLa cells and MCF-7 cells are taken on an inverted fluorescent microscope (Nikon, Japan). MTT assay is measured using a Synergy H1 ELISA plate reader at 490 nm (BioTek, USA).

Preparation of Octa-aminopropyl Polyhedral Oligomeric Silsesquioxane Hydrochloride Salt. Octa-aminopropyl polyhedral oligomeric silsesquioxane hydrochloride salt (OA-POSS) is prepared by following a previously reported procedure.[37] Briefly, 30 mL of APTES and 240 mL of methanol are mixed thoroughly in a 500 mL closed round-bottom flask after stirring for 3 min. Then, 40.5 mL of hydrochloric acid (36.5%, m/v) is added drop-wise into the mixture. After vigorous stirring for 7 days at room temperature in a closed flask, white precipitate is obtained. The product is washed by methanol 3 times to remove excess APTES and hydrochloric acid. Finally, OA-POSS powder is collected after vacuum drying at 60 °C overnight. OA-POSS is stored in a sealed vessel for further use.

Preparation of OA-POSS Functionalized Carbon Dots (CDs/POSS). First, 50 mL of glycerol and various amounts of OA-POSS (25, 50, 100, 125, 150, 300, and 500 mg) are mixed thoroughly in a 100 mL round-bottom flask, separately. After ultrasonication for 2 h, the mixture is heated and stirred on an electric heating mantle by refluxing at 230 °C for 12 h. During the reaction process, it is noticed that the colorless solution gradually turns into dark brown syrup. After cooling to room temperature, the reaction mixture is diluted with 500 mL of pure water. The CDs/POSS is collected by further purification with dialysis against pure water with cellulose ester membrane (MWCO: 500−1000) for 72 h to remove any unreacted/residual glycerol and OA-POSS.

Cell Imaging and Cellular Toxicity Test. The practical applications of CDs/POSS have been demonstrated by fluorescence imaging of HeLa cells and MCF-7 cells. The operating procedures include HeLa cells/MCF-7 cells incubated with DMEM high glucose medium containing 10% fetal bovine serum, 100 units mL^{-1} penicillin, and 100 mg mL^{-1} streptomycin at 37 °C with 5% CO_2 in a humidified incubator for 24 h. Subsequently, the medium is removed, and HeLa cells are washed gently with PBS buffer (10 mmol L^{-1}, pH 7.4) three times. Afterward, HeLa/MCF-7 cells are cultured for 6 h in the medium containing 5 mg mL^{-1} of CDs/POSS which has been filtered through a 0.22 μm sterilized filter membrane before use. After being washed with PBS buffer three times, the fluorescence images are taken on an inverted fluorescent microscope with laser excitation at 340 and 495 nm.

The cytotoxicity and biocompatibility of CDs/POSS are evaluated by carrying out MTT assay. At first, HeLa/MCF-7 cells are seeded in a 96-well culture plate. After incubation for 12 h, CDs/POSS (in 10 mmol L^{-1} PBS buffer, pH 7.4) with various concentrations (0.2, 0.5, 1.0, 2.0, 3.0, 4.0, 5.0, 6.0, and 7.0 mg mL^{-1}) are added into the cells and incubated for 20 h at 37 °C with 5% CO_2. Then, 20 μL MTT (5 mg mL^{-1}) is added into each well, and the plate is further incubated for an additional 4 h for deoxidizing MTT. After that, the medium is aspirated out, and 150 μL DMSO is added into each well to facilitate the dissolution of formazan. Control experiments are carried out under the same incubation conditions in the absence of CDs/POSS. The absorbance of each well is measured at 490 nm by ELISA plate reader.

RESULTS AND DISCUSSION

Mechanisms for the Formation of Carbon Dots (CDs/POSS). Scheme 1A illustrates the formation of OA-POSS via hydrolytic condensation of APTES with hydrochloric acid acting as catalyst. The production of carbon dots (CDs/POSS)

Scheme 1. (A) Schematic Illustration for the Hydrolytic Condensation of APTES to Produce OA-POSS and (B) Preparation of Carbon Dots (CDs/POSS) with Glycerol As Carbon Source and Solvent Medium and OA-POSS As Passivation Agent

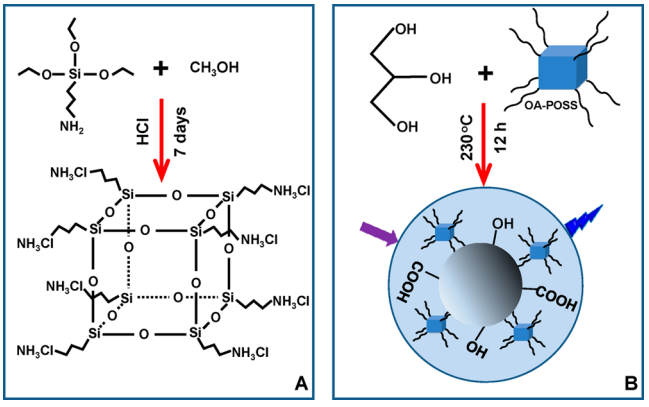

DOI: 10.1021/acsami.5b04172
ACS Appl. Mater. Interfaces 2015, 7, 16609−16616

is schematically shown in Scheme 1B. It is known that the "glycerol−oxygen" reaction is a key step for the preparation of carbon dots,[22] and thus, the reaction is carried out in an open system. In this process, dehydration and carbonization of glycerol are taking place. As reported in a previous work,[39] the pyrolysis process involves dehydration and fragmentation of glycerol, where the major products include 2-propenal, acetaldehyde, and formaldehyde which are generated at a relatively low temperature at the beginning of the reaction. Meanwhile, the hydrogen atoms of OA-POSS and the hydroxyl groups in glycerol could be involved in the dehydration process.[40] In this respect, the presence of H_2O molecule provides a proof for the dehydration of glycerol. In addition, glycerol dehydration accelerates the process of carbonization. 2-Propenal, acetaldehyde, and formaldehyde tend to be carbonized at a higher temperature of ca. 230 °C and decomposed to C−C and C═C bonds, leading to the formation of carbogenic core. On the other hand, carboxylic groups are formed on the bare carbon dots, which are then passivated with amino groups in OA-POSS, and this endows the obtained CDs/POSS with favorable hydrophilicity. After adding excessive amount of $AgNO_3$ solution, no precipitation is found in the CDs/POSS solution, indicating that Cl^- on OA-POSS may volatilize in the form of HCl during the passivation process.

Generally, when glycerol is used as carbon source for the formation of CDs, phosphate salt usually serves as a catalyst.[41] In the present work, however, phosphate salt is not involved, and thus, OA-POSS takes over the role of the catalyst besides serving as the passivation agent.

Characterizations of OA-POSS and Carbon Dots (CDs/POSS). For the purpose of evaluating the formation of CDs/POSS and providing support for the mechanisms discussed in the previous section, the following characterizations with XPS and FT-IR analyses are performed.

In the FT-IR spectra of OA-POSS, the absorption bands at 3432 and 1600 cm^{-1} (Figure 1) are assigned to $-NH_3^+$

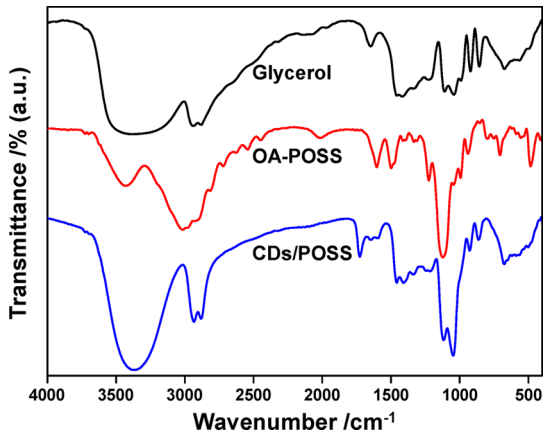

Figure 1. FT-IR spectra of glycerol, OA-POSS, and CDs/POSS.

stretching and bending vibrations, respectively. The absorptions at 1120 and 1042 cm^{-1} are identified and ascribed to the asymmetric stretching vibrations of Si−O−Si, and those at 560 and 475 cm^{-1} are due to the deformation vibrations of POSS skeletal, which clearly demonstrated the formation of Si−O−Si framework. In addition, the absorption band at 700 cm^{-1} is attributed to the stretching vibration of Si−C, and the stretching vibration of C−N is identified at 1225 cm^{-1}. The information provided by FT-IR analysis well illustrated the formation of OA-POSS.

To further verify the structure of OA-POSS, ^1H NMR, ^{13}C NMR and ^{29}Si NMR spectra are presented in Figure S1. For ^1H NMR spectrum (Figure S1A, Supporting Information), the chemical shifts at 0.73, 1.74, 2.79, and 8.26 ppm are assigned to $-CH_2Si$, $-CH_2-$, $-CH_2NH_3Cl$ and $-NH_3Cl$, respectively. ^{13}C NMR (Figure S1B, Supporting Information) peaks at 8.87, 21.05, and 41.45 ppm are ascribed to $-CH_2Si$, $-CH_2-$, and $-CH_2NH_3Cl$, respectively. A sharp solo peak at −66.5 ppm in ^{29}Si NMR spectrum (Figure S1C, Supporting Information) is attributed to Si atom on the inorganic cubic core of OA-POSS, reflecting that Si−O−Si structure has been formed via hydrolytic condensation.

For the case of the obtained carbon dots (CDs/POSS), the characteristic absorption bands of OA-POSS attributed to the asymmetric stretching vibrations of Si−O−Si are clearly identified at 1120 and 1049 cm^{-1}. The broad and intense absorption bands at 3365 cm^{-1} are assigned to the stretching vibrations of hydrophilic groups $-NH_2$ and −OH (e.g., the residual hydroxyl groups of glycerol and those on carboxylic acid). This corresponds to the favorable solubility of the CDs/POSS in aqueous medium. The absorption band at 1585 cm^{-1} is ascribed to the N−H bending vibration, and those at 2934 and 2879 cm^{-1} are due to the C−H stretching vibrations. It is worth noting herein that the characteristic absorption at 1651 cm^{-1} is identified as −C═O stretching vibration on amide, which proves that bare CDs have been successfully bound to OA-POSS via amide linkage. Meanwhile, the absorption at 1732 cm^{-1} is attributed to C═O on carboxylic acid groups. This indicates that carboxylic groups have been partially converted into amide groups, while the left remains unchanged during the process of passivation by OA-POSS.

XPS analysis provides further information on the surface composition and elemental analysis of OA-POSS and CDs/POSS. Their XPS spectra are given in Figures 2 and 3. It is seen that OA-POSS exhibits four typical peaks corresponding to C, N, Si and O, and the atomic percentage of these elements are 59.76, 8.21, 12.83, and 19.19%. N spectrum is ascribed to C−N bonding from alkyl ammonium at 401.1 eV, and C spectrum consists of three peaks at 284.5, 284.8, and 286.0 eV, attributed to C−C, C−Si, and C−N bonds. In addition, Si spectrum exhibits two fitted peaks at 101.6 and 102.4 eV, which can be assigned to Si−C and Si−O groups. The fitted solo peak in O spectrum at 532.0 eV is attributed to the O−Si groups on the inorganic core of OA-POSS.

In comparison with OA-POSS, obvious changes have been located in the XPS spectra of CDs/POSS, illustrating three predominant peaks for C, Si and O in Figure 3. The small peak of N can still be identified, and the atomic percentage for C, N, Si, and O are derived to be 73, 0.89, 1.08, and 25.03%. The increase in carbon content indicates the formation of carbogenic core, meanwhile, the existence of N and Si well illustrates that OA-POSS has been bound onto CDs. The N_{1s} spectrum reveals the presence of alkyl ammonium C−N bond at 401.4 eV, and the alkyl amide C−N bond at 399.6 eV further confirms the combination of OA-POSS with carbon dots. The O 1s shows a new peak at 531.6 eV due to C═O bonding of carbonyl. On the other hand, the C spectrum can be deconvoluted into five peaks, except for the original three peaks of OA-POSS, two new peaks are identified with binding energies at 286.7 and 288.5 eV, corresponding to C−O and

DOI: 10.1021/acsami.5b04172
ACS Appl. Mater. Interfaces 2015, 7, 16609−16616

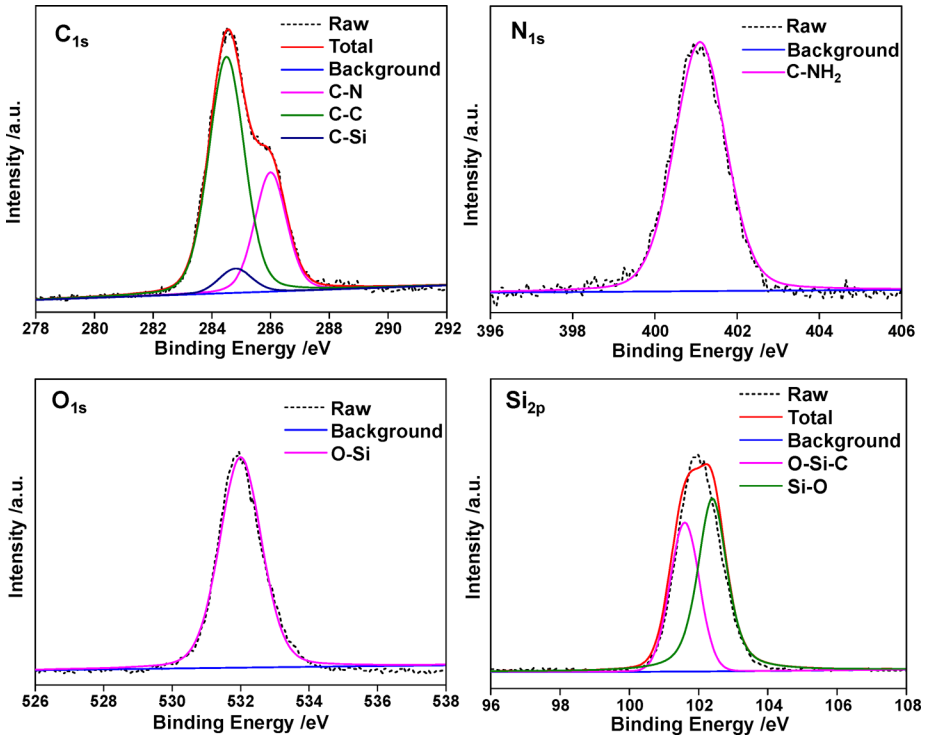

Figure 2. XPS spectra of OA-POSS illustrating high resolution peaks for C_{1s}, N_{1s}, O_{1s}, and Si_{2p}.

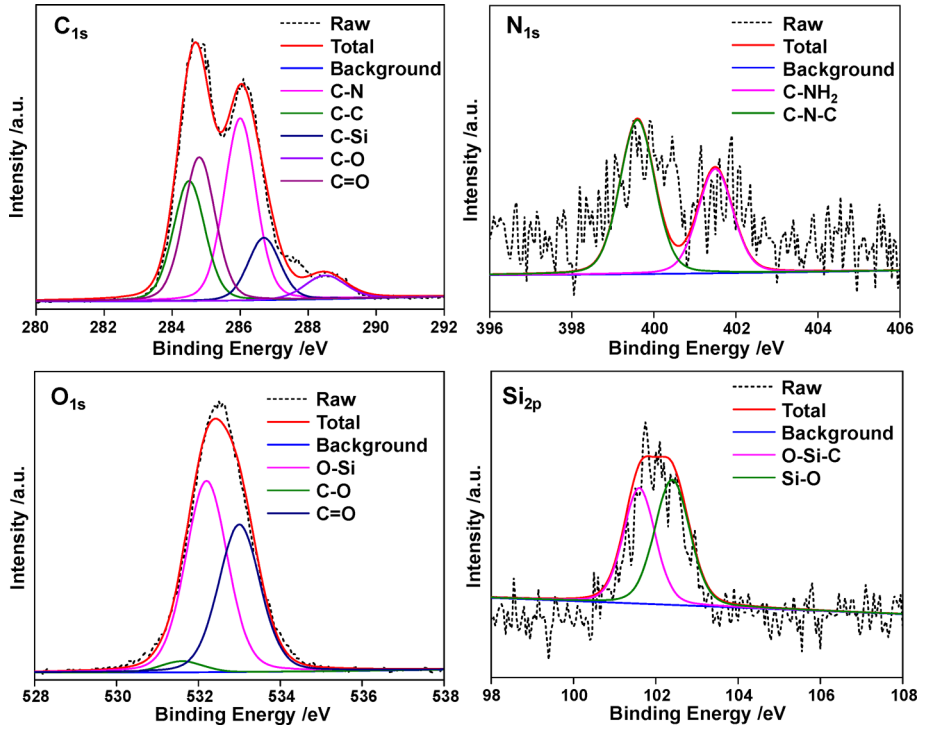

Figure 3. XPS spectra of the carbon dots (CDs/POSS) illustrating high resolution peaks for C_{1s}, N_{1s}, O_{1s}, and Si_{2p}.

C═O bonds. In addition, no change is observed for the Si spectrum with respect to that for OA-POSS.

Overall, the XPS analysis results are consistent with those of FT-IR, which further demonstrated the fabrication of OA-POSS on the surface of CDs.

TGA curve for the OA-POSS (Figure S2, Supporting Information) illustrates a slight weight loss of 5.6% attributed to the evaporation of water molecules. Then, a sharp decrease is observed from 280 to 400 °C due to the decomposition of aminopropyl groups on the arms of the OA-POSS. At 800 °C, ca. 40% residue is still left, which is supposed to be attributed to the Si−O−Si inorganic core. On the other hand, the POSS functionalized carbon dots (CDs/POSS) exhibit favorable thermal stability at <230 °C, while subsequently in the range of 230−280 °C, a weight loss of 24.8% is observed, corresponding to the pyrolysis of the carbogenic core. A

DOI: 10.1021/acsami.5b04172
ACS Appl. Mater. Interfaces 2015, 7, 16609−16616

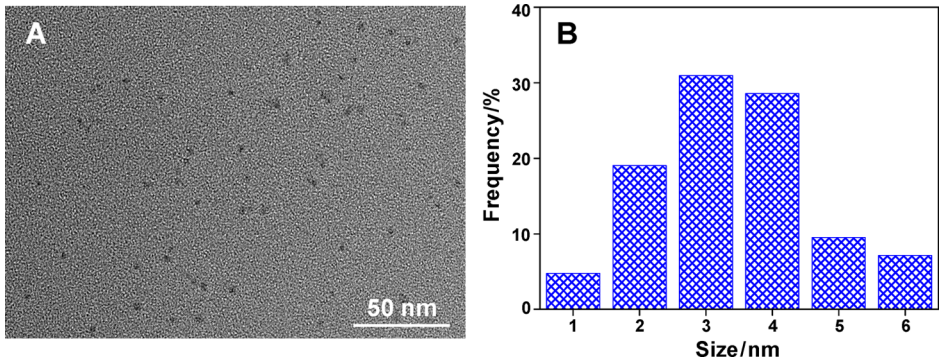

Figure 4. (A) HRTEM images and (B) particle size distribution for the carbon dots (CDs/POSS).

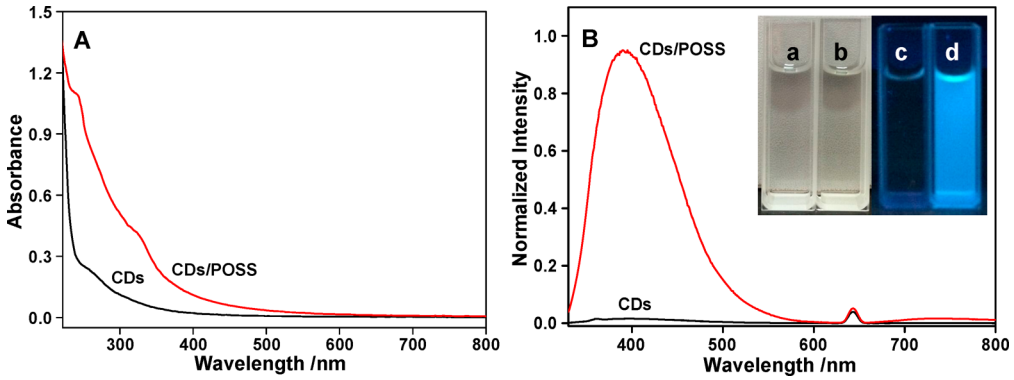

Figure 5. (A) UV−vis spectra and (B) fluorescence spectra for the bare CDs and POSS functionalized carbon dots (CDs/POSS). (B, inset, a and c) Bare CDs under visible and UV light and (b and d) POSS functionalized carbon dots (CDs/POSS) under visible and UV light.

similar weight loss is encountered within 280−400 °C as that observed for OA-POSS due to the degradation of surface functional groups (aminopropyl groups). As the temperature rises to 500−800 °C, the TGA curve levels off with a 9.2% residue of the original weight attributed to the Si−O−Si core.

TEM images in Figure 4A show that the POSS functionalized carbon dots (CDs/POSS) are well dispersed in aqueous medium with diameter distribution in a range of 1−6 nm (Figure 4B), and an average particle size of ca. 3.6 nm is obtained.

Photoluminescent Property of POSS Functionalized Carbon Dots (CDs/POSS). UV−vis absorbance spectra for the carbon dots (CDs/POSS) in Figure 5A show a relatively strong absorption within 200−400 nm with two characteristic peaks. The absorption at 240 nm is attributed to the $\pi-\pi^*$ transition of aromatic sp^2 domains,[42] while the other at 320 nm is attributed to the $n-\pi^*$ transition of C═O bond, which is similar to that reported for common CDs at 340 nm.[5] The aqueous solution of CDs/POSS is yellowish under visible light, while it emits bright blue photoluminescence under UV lamp at 365 nm as illustrated in Figure 5B. As shown in Figure 6, when the excitation wavelength is varied from 320 to 420 nm, the maximum emission wavelength shifts from 400 to 490 nm, along with significant variation of the fluorescence intensity. This excitation dependent emission wavelength and fluorescence intensity provide a potential for multicolor imaging applications. The maximum fluorescence emission intensity could be obtained by excitation at 320 nm, with a full width at half-maximum (fwhm) of ca. 100 nm, which is approximately the same as that for the most reported carbon dots.[22,43] Although the mechanisms for photoluminescence behaviors of carbon dots are still under debate, this excitation wavelength-dependent phenomenon could be explained by the size distribution of CDs/POSS and the considerable distribution of emissive traps on the surface of CDs/POSS, as suggested in a previous report.[44]

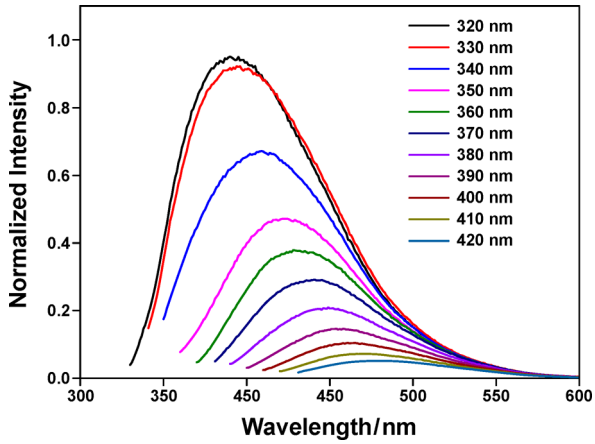

Figure 6. Fluorescence spectra of the POSS functionalized carbon dots (CDs/POSS) with excitation wavelength in the range of 320−420 nm (with an interval of 10 nm).

The quantum yield (QY) of POSS functionalized carbon dots (CDs/POSS) achieved by using different amounts of OA-POSS at the maximum excitation wavelength of 320 nm are measured with quinine sulfate in 0.05 mol L^{-1} H_2SO_4 (QY, 54%) as a reference standard, and the results are shown in Figure S3 (Supporting Information). It is seen that at the beginning an improvement on the QY of CDs/POSS is observed with the increase of the amount of OA-POSS applied.

DOI: 10.1021/acsami.5b04172
ACS Appl. Mater. Interfaces 2015, 7, 16609−16616

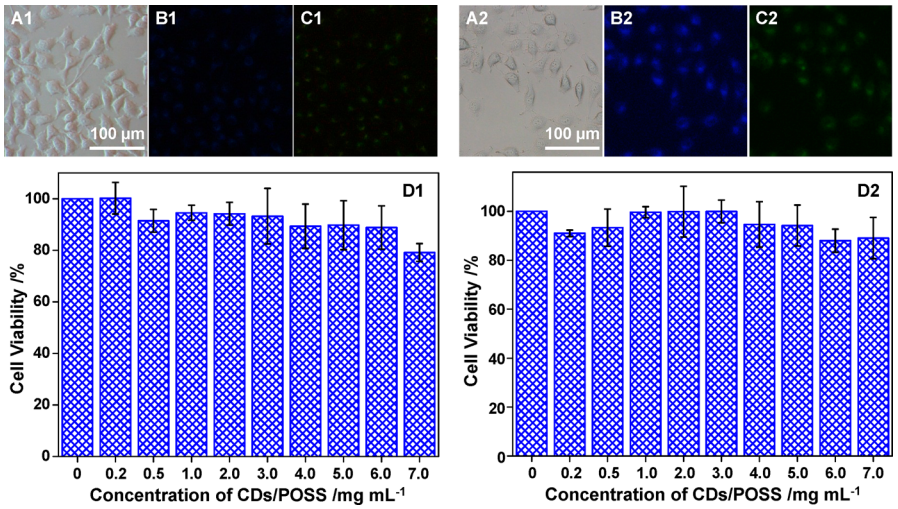

Figure 7. Fluorescent microscope images of (A1–D1) HeLa cells and (A2–D2) MCF-7 cells labeled with CDs/POSS. (A1 and A2) Bright field images; (B1 and B2) with an excitation wavelength at 340 nm; (C1 and C2) with an excitation wavelength at 495 nm; and (D1 and D2) viability of HeLa cells and MCF-7 cells incubated with different concentrations of CDs/POSS.

A QY of 24.0% is achieved for the CDs/POSS when 125 mg of OA-POSS is added into the reaction system for CDs functionalization/passivation. This QY is obviously much higher than that of most of the CDs prepared with glycerol as carbon source.[22,41,42]

It was reported previously that surface passivation is among the major contribution to the strong fluorescence of carbon dots.[16,42,45] In the present study, a parallel control experiment is carried out, and consistent results are observed. First, 50 mL of glycerol is used as carbon source and heated at 230 °C for 12 h to produce bare CDs. As expected, the results in Figure 5B illustrate a very low fluorescence intensity for the bare CDs, and a slight emission is observed under UV light at 365 nm. The quantum yield for bare CDs is derived to be 2.61%, at approximately the same level as that reported in the literature.[40] The present study has demonstrated that OA-POSS passivation is the main cause for the improvement on quantum yield of the CDs/POSS, which passivates the "defect sites" located on the surface of the bare CDs.

Stability of CDs/POSS. As illustrated in Figure S4 (Supporting Information), the CDs/POSS exhibit stable photoluminescence within a wide pH range (e.g., pH 3–11). However, in a strong acidic or basic medium (e.g., pH < 2 and pH > 12), a sharp decrease of the fluorescence intensity is encountered. This pH-dependent photoluminescent behavior is similar to that reported in a previous work,[46] which can be explained by protonation and deprotonation of −COOH/−NH_2 groups on the surface of CDs/POSS.[47] A previous work indicated that carboxylic groups exist in the form of $-COO^-$ in neutral and alkaline media, while amine groups tend to form $-NH_3^+$ in acidic and neutral environment.[48] At pH 3–11, $-COO^-$ is completely neutralized by $-NH_3^+$, and the surface chemistry of CDs/POSS is stable with charge neutrality, PL intensity reaches at a stable maximum level. At pH < 3, −COOH/$-NH_2$ groups are protonated, some electrons are captured by the positively charged centers on the surface, photoexcited electron–hole pairs are generated, resulting in gradual drop of the PL intensity with decrease of pH value.[49] At pH > 11, the surface of CDs/POSS is negatively charged as a result of the depronation of −COOH/$-NH_2$ groups, a "protective shell" with a negative charge is formed on the surface of CDs/POSS with ineffective radiative recombination,[50] and the PL intensity decreases.

For the purpose of evaluating the effect of ionic strength on the fluorescence intensity, 0–1.0 mol L^{-1} NaCl is added into the CDs/POSS aqueous solution in 10 mM PBS (pH 7.4), and the results are given in Figure S5 (Supporting Information). It is seen that ionic strength at certain level poses virtually no effect on the photoluminescence of CDs/POSS.

The photoluminescent behaviors of CDs/POSS in the presence of metal cations, especially heavy metal species such as Cd^{2+}, Hg^{2+}, Cr(VI), As(III), As(V), and Pb^{2+}, have been investigated and the results are given in Figure S6 (Supporting Information). Ten milligrams per liter (10 mg L^{-1}) of the tested metal cations pose no effect on the photoluminescence of CDs/POSS. On the other hand, considering that some organic molecules (e.g., hemin, ascorbic acid, L-cysteine, glycine, phenylalanine, uric acid and vitamin B12) are widely found in biological systems, their effect on the photoluminescent property of CDs/POSS is investigated, and the results are illustrated in Figure S7 (Supporting Information). It seems that these organic molecules have no obvious effect on the photoluminescent behaviors of CDs/POSS.

In addition, the fluorescence intensity of CDs/POSS has been recorded under continuous excitation at 320 nm for 3600 s. The results given in Figure S8 (Supporting Information) well demonstrated that the CDs/POSS exhibit favorable resistance to photobleaching.

Cell Imaging and Cellular Toxicity Test. The cytotoxicity of CDs/POSS has been investigated by incubating HeLa cells and MCF-7 cells in the presence of CDs/POSS at the concentration level of 0.2–7.0 mg mL^{-1}. The experimental results in Figure 7D1,D2 indicated that cell viability of >90% (HeLa cells) and >94% (MCF-7 cells) are achieved at a CDs/POSS concentration of <5.0 mg mL^{-1} and incubating for 6 h. The viability of cells are still maintained at >80% for HeLa cells and >89% for MCF-7 cells at a concentration level of 7.0 mg mL^{-1} CDs/POSS. These observations demonstrated low cytotoxicity or favorable biocompatibility for the CDs/POSS and thus provide a potential for biological application (e.g., cell imaging). Figure 7 illustrates the HeLa/MCF-7 cell imaging results after incubating them with 5 mg mL^{-1} of CDs/POSS for

DOI: 10.1021/acsami.5b04172
ACS Appl. Mater. Interfaces 2015, 7, 16609–16616

6 h. It is obvious that with laser excitation at 340 and 495 nm, respectively, bright blue and green emissions are clearly recorded on the fluorescent microscope, while no visible fluorescence emission is detected in the control experiments (Figure S9, Supporting Information). This observation indicates that the POSS functionalized carbon dots have been up-taken by HeLa cells and MCF-7 cells. Furthermore, favorable biocompatibility is found for CDs/POSS with respect to other carbon materials at high concentration, for example, mesoporous carbon nanosphere,[51] carbon nanoparticles,[13] and graphene quantum dots.[52]

CONCLUSIONS

We have constructed organic−inorganic hybrid carbon dots, namely, octa-aminopropyl polyhedral oligomeric silsesquioxane (OA-POSS) functionalized carbon dots (CDs/POSS), by one pot method. OA-POSS serves as passivation agent and the functionalization provides CDs/POSS a high quantum yield of 24.0%, in addition to favorable biocompatibility. They also exhibit resistance to photobleaching and excellent photoluminescence stability in the presence of biological sample matrix, which facilitate cell imaging in biological systems. In addition, the excitation wavelength-dependent emission wavelength and fluorescence intensity well facilitates multicolor imaging applications. The present study offers a useful approach for the development of photoluminescent probe for the application in biological imaging.

ASSOCIATED CONTENT

Supporting Information

^{1}H NMR, ^{13}C NMR, and ^{29}Si NMR spectra of OA-POSS. TG curves of OA-POSS and CDs/POSS, the QY of CDs/POSS by using various amounts of OA-POSS during the passivation process, the effect of pH value, ionic strength, metal cations, organic molecules and irradiation time on the fluorescence intensity of CDs/POSS, fluorescent microscope images of HeLa cells and MCF-7 cells without labeling are presented. The Supporting Information is available free of charge on the ACS Publications website at DOI: 10.1021/acsami.5b04172.

AUTHOR INFORMATION

Corresponding Authors

*E-mail: chenml@mail.neu.edu.cn.

*E-mail: jianhuajrz@mail.neu.edu.cn. Tel: +86 24 83688944. Fax: +86 24 83676698.

Notes

The authors declare no competing financial interest.

ACKNOWLEDGMENTS

The authors appreciate financial support from the Natural Science Foundation of China (21275027, 21235001, and 21475017), the SRFDP program (20120042110020), Liaoning Provincial Natural Science Foundation (2014020041), and Fundamental Research Funds for the Central Universities (N140505003, N141008001).

REFERENCES

(1) Cao, L.; Wang, X.; Meziani, M. J.; Lu, F. S.; Wang, H. F.; Luo, P. J. G.; Lin, Y.; Harruff, B. A.; Veca, L. M.; Murry, D.; Xie, S. Y.; Sun, Y. P. Carbon Dots for Multiphoton Bioimaging. *J. Am. Chem. Soc.* **2007**, *129*, 11318−11319.

(2) Li, W.; Zhang, Z. H.; Kong, B. A.; Feng, S. S.; Wang, J. X.; Wang, L. Z.; Yang, J. P.; Zhang, F.; Wu, P. Y.; Zhao, D. Y. Simple and Green Synthesis of Nitrogen-Doped Photoluminescent Carbonaceous Nanospheres for Bioimaging. *Angew. Chem., Int. Ed.* **2013**, *52*, 8151−8155.

(3) Choi, Y.; Kim, S.; Choi, M. H.; Ryoo, S. R.; Park, J.; Min, D. H.; Kim, B. S. Highly Biocompatible Carbon Nanodots for Simultaneous Bioimaging and Targeted Photodynamic Therapy In Vitro and In Vivo. *Adv. Funct. Mater.* **2014**, *24*, 5781−5789.

(4) Zhu, A. W.; Qu, Q.; Shao, X. L.; Kong, B.; Tian, Y. Carbon-Dot-Based Dual-Emission Nanohybrid Produces a Ratiometric Fluorescent Sensor for In Vivo Imaging of Cellular Copper Ions. *Angew. Chem., Int. Ed.* **2012**, *124*, 7185−7189.

(5) Zheng, M.; Xie, Z. G.; Qu, D.; Li, D.; Du, P.; Jing, X. B.; Sun, Z. C. On-Off-On Fluorescent Carbon Dot Nanosensor for Recognition of Chromium(VI) and Ascorbic Acid Based on the Inner Filter Effect. *ACS Appl. Mater. Interfaces* **2013**, *5*, 13242−13247.

(6) Li, L. B.; Wang, C.; Liu, K. Y.; Wang, Y. H.; Liu, K.; Lin, Y. Q. Hexagonal Cobalt Oxyhydroxide-Carbon Dots Hybridized Surface: High Sensitive Fluorescence Turn-on Probe for Monitoring of Ascorbic Acid in Rat Brain Following Brain Ischemia. *Anal. Chem.* **2015**, *87*, 3404−3411.

(7) Guo, X.; Wang, C. F.; Yu, Z. Y.; Chen, L.; Chen, S. Facile Access to Versatile Fluorescent Carbon Dots toward Light-Emitting Diodes. *Chem. Commun.* **2012**, *48*, 2692−2694.

(8) Li, H. T.; He, X. D.; Kang, Z. H.; Huang, H.; Liu, Y.; Liu, J. J.; Lian, S. Y.; Tsang, C. H.; Yang, X. B.; Lee, S. T. Water-Soluble Fluorescent Carbon Quantum Dots and Photocatalyst Design. *Angew. Chem., Int. Ed.* **2010**, *49*, 4430−4434.

(9) Baker, S. N.; Baker, G. A. Luminescent Carbon Nanodots: Emergent Nanolights. *Angew. Chem., Int. Ed.* **2010**, *49*, 6726−6744.

(10) Liu, H. P.; Ye, T.; Mao, C. D. Fluorescent Carbon Nanoparitcles Derived from Candle Soot. *Angew. Chem., Int. Ed.* **2007**, *46*, 6473−6475.

(11) Sun, Y. P.; Zhou, B.; Lin, Y.; Wang, W.; Fernando, K. A. S.; Pathak, P.; Meziani, M. J.; Harruff, B. A.; Wang, X.; Wang, H. F.; Luo, P. J. G.; Yang, H.; Kose, M. E.; Chen, B. L.; Veca, L. M.; Xie, S. Y. Quantum-Sized Carbon Dots for Bright and Colorful Photoluminescence. *J. Am. Chem. Soc.* **2006**, *128*, 7756−7757.

(12) Zhou, J. G.; Booker, C.; Li, R. Y.; Zhou, X. T.; Sham, T. K.; Sun, X. L.; Ding, Z. F. An Electrochemical Avenue to Blue Luminescent Nanocrystals from Multiwalled Carbon Nanotubes (MWCNTs). *J. Am. Chem. Soc.* **2007**, *129*, 744−745.

(13) Shen, L. M.; Zhang, L. P.; Chen, M. L.; Wang, J. H. The Production of pH-sensitive Photoluminescent Carbon Nanoparticles by the Carbonization of Polyethylenimine. *Carbon* **2013**, *55*, 343−349.

(14) Lin, X. M.; Gao, G. M.; Zheng, L. Y.; Chi, Y. W.; Chen, G. N. Encapsulation of Strongly Fluorescent Carbon Quantum Dots in Metal-Organic Frameworks for Enhancing Chemical Sensing. *Anal. Chem.* **2014**, *86*, 1223−1228.

(15) Zong, J.; Zhu, Y. H.; Yang, X. L.; Shen, J. H.; Li, C. Z. Synthesis of Photoluminescent Carbogenic Dots Using Mesoporous Silica Spheres as Nanoreactors. *Chem. Commun.* **2011**, *47*, 764−766.

(16) Qiao, Z. A.; Wang, Y. F.; Gao, Y.; Li, H. W.; Dai, T. Y.; Liu, Y. L.; Huo, Q. S. Commercially Activated Carbon as the Source for Producing Multicolor Photoluminescent Carbon Dots by Chemical Oxidation. *Chem. Commun.* **2010**, *46*, 8812−8814.

(17) De, B.; Karak, N. A Green and Facile Approach for the Synthesis of Water Soluble Fluorescent Carbon Dots from Banana Juice. *RSC Adv.* **2013**, *3*, 8286−8290.

(18) Sahu, S.; Behera, B.; Maiti, T. K.; Mohapatra, S. Simple One-Step Synthesis of Highly Luminescent Carbon Dots from Orange Juice: Application as Excellent Bio-Imaging Agents. *Chem. Commun.* **2012**, *48*, 8835−8837.

(19) Park, S. Y.; Lee, H. U.; Park, E. S.; Lee, S. C.; Lee, J. W.; Jeong, S. W.; Kim, C. H.; Lee, Y. C.; Huh, Y. S.; Lee, J. Photoluminescent Green Carbon Nanodots from Food-Waste-Derived Sources: Large-Scale Synthesis, Properties, and Biomedical Applications. *ACS Appl. Mater. Interfaces* **2014**, *6*, 3365−3370.

(20) Wang, L.; Zhou, H. S. Green Synthesis of Luminescent Nitrogen-Doped Carbon Dots from Milk and Its Imaging Application. *Anal. Chem.* **2014**, *86*, 8902−8905.

DOI: 10.1021/acsami.5b04172
ACS Appl. Mater. Interfaces 2015, 7, 16609−16616

(21) Zhang, J.; Yuan, Y.; Liang, G. L.; Yu, S. H. Scale-Up Synthesis of Fragrant Nitrogen-Doped Carbon Dots from Bee Pollens for Bioimaging and Catalysis. *Adv. Sci.* **2015**, *2*, 1500002.
(22) Lai, C. W.; Hsiao, Y. H.; Peng, Y. K.; Chou, P. T. Facile Synthesis of Highly Emissive Carbon Dots from Pyrolysis of Glycerol; Gram Scale Production of Carbon Dots/mSiO$_2$ for Cell Imaging and Drug Release. *J. Mater. Chem.* **2012**, *22*, 14403−14409.
(23) Peng, H.; Travas-Sejdic, J. Simple Aqueous Solution Route to Luminescent Carbogenic Dots from Carbohydrates. *Chem. Mater.* **2009**, *21*, 5563−5565.
(24) Jaiswal, A.; Ghosh, S. S.; Chattopadhyay, A. One Step Synthesis of C-dots by Microwave Mediated Caramelization of Poly(ethylene glycol). *Chem. Commun.* **2012**, *48*, 407−409.
(25) Cao, L.; Meziani, M. J.; Sahu, S.; Sun, Y. P. Photoluminescence Properties of Graphene versus Other Carbon Nanomaterials. *Acc. Chem. Res.* **2013**, *46*, 171−180.
(26) Fowley, C.; McCaughan, B.; Devlin, A.; Yildiz, I.; Raymo, F. M.; Callan, J. F. Highly Luminescent Biocompatible Carbon Quantum Dots by Encapsulation with an Amphiphilic Polymer. *Chem. Commun.* **2012**, *48*, 9361−9363.
(27) Dong, Y. Q.; Wang, R. X.; Li, H.; Shao, J. W.; Chi, Y. W.; Lin, X. M.; Chen, G. N. Polyamine-Functionalized Carbon Quantum Dots for Chemical Sensing. *Carbon* **2012**, *50*, 2810−2815.
(28) Shi, Q. Q.; Li, Y. H.; Xu, Y.; Wang, Y.; Yin, X. B.; He, X. W.; Zhang, Y. K. High-Yield and High-Solubility Nitrogen-Doped Carbon Dots: Formation, Fluorescence Mechanism and Imaging Application. *RSC Adv.* **2014**, *4*, 1563−1566.
(29) Wang, W. P.; Lu, Y. C.; Huang, H.; Wang, A. J.; Chen, J. R.; Feng, J. J. Facile Synthesis of N, S-codoped Fluorescent Carbon Nanodots for Fluorescent Resonance Energy Transfer Recognition of Methotrexate with High Sensitivity and Selectivity. *Biosens. Bioelectron.* **2015**, *64*, 517−522.
(30) Kannan, R. Y.; Salacinski, H. J.; De Groot, J.; Clatworthy, I.; Bozec, L.; Horton, M.; Butler, P. E.; Seifalian, A. M. The Antithrombogenic Potential of a Polyhedral Oligomeric Silsesquioxane (POSS) Nanocomposite. *Biomacromolecules* **2006**, *7*, 215−223.
(31) McCusker, C.; Carroll, J. B.; Rotello, V. M. Cationic Polyhedral Oligomeric Silsesquioxane (POSS) Units as Carriers for Drug Delivery Processes. *Chem. Commun.* **2005**, *8*, 996−998.
(32) Zhang, L.; Abbenhuis, H. C. L.; Yang, Q. H.; Wang, Y. M.; Magusin, P. C. M. M.; Mezari, B.; van Santen, R. A.; Li, C. Mesoporous Organic-Inorganic Hybrid Materials Built Using Polyhedral Oligomeric Silsesquioxane Blocks. *Angew. Chem.* **2007**, *119*, 5091−5094.
(33) Pu, K. Y.; Li, K.; Zhang, X. H.; Liu, B. Conjugated Oligoelectrolyte Harnessed Polyhedral Oligomeric Silsesquioxane as Light-Up Hybrid Nanodot for Two-Photon Fluorescence Imaging of Cellular Nucleus. *Adv. Mater.* **2010**, *22*, 4186−4189.
(34) Wang, Y.; Vaneski, A.; Yang, H. H.; Gupta, S.; Hetsch, F.; Kershaw, S. V.; Teoh, W. Y.; Li, H. R.; Rogach, A. L. Polyhedral Oligomeric Silsesquioxane as a Ligand for CdSe Quantum Dots. *J. Phys. Chem. C* **2013**, *117*, 1857−1862.
(35) Li, L. G.; Feng, S. Y.; Liu, H. Z. Hybrid Lanthanide Complexes Based on a Novel β-Diketone Functionalized Polyhedral Oligomeric Silsesquioxane (POSS) and Their Nanocomposites with PMMA via in Situ Polymerization. *RSC Adv.* **2014**, *4*, 39132−39139.
(36) Chen, X. F.; Zhang, P. N.; Wang, T. R.; Li, H. R. The First Europium(III) β-Diketonate Complex Functionalized Polyhedral Oligomeric Silsesquioxane. *Chem. - Eur. J.* **2014**, *20*, 2551−2556.
(37) He, Y.; Wang, H. F.; Yan, X. P. Self-Assembly of Mn-Doped ZnS Quantum Dots/Octa(3-aminopropyl)octasilsequioxane Octahydrochloride Nanohybrids for Optosensing DNA. *Chem. - Eur. J.* **2009**, *15*, 5436−5440.
(38) Zhao, X.; Zhang, W. J.; Wu, Y. Z.; Liu, H. Z.; Hao, X. P. Facile Fabrication of OA-POSS Modified Near-Infrared-Emitting CdSeTe Alloyed Quantum Dots and their Bioapplications. *New J. Chem.* **2014**, *38*, 3242−3249.
(39) Nimlos, M. R.; Blanksby, S. J.; Qian, X. H.; Himmel, M. E.; Johnson, D. K. Mechanisms of Glycerol Dehydration. *J. Phys. Chem. A* **2006**, *110*, 6145−6156.
(40) Mao, L. H.; Tang, W. Q.; Deng, Z. Y.; Liu, S. S.; Wang, C. F.; Chen, S. Facile Access to White Fluorescent Carbon Dots toward Light Emitting Devices. *Ind. Eng. Chem. Res.* **2014**, *53*, 6417−6425.
(41) Wang, X. H.; Qu, K. G.; Xu, B. L.; Ren, J. S.; Qu, X. G. Microwave Assisted One-Step Green Synthesis of Cell-Permeable Multicolor Photoluminescent Carbon Dots without Surface Passivation Reagents. *J. Mater. Chem.* **2011**, *21*, 2445−2450.
(42) Pan, D. Y.; Zhang, J. C.; Li, Z.; Wu, M. H. Hydrothermal Route for Cutting Graphene Sheets into Blue-Luminescent Graphene Quantum Dots. *Adv. Mater.* **2010**, *22*, 734−738.
(43) Liu, C. J.; Zhang, P.; Tian, F.; Li, W. C.; Li, F.; Liu, W. G. One-step Synthesis of Surface Passivated Carbon Nanodots by Microwave Assisted Pyrolysis for Enhanced Multicolor Photoluminescence and Bioimaging. *J. Mater. Chem.* **2011**, *21*, 13163−13167.
(44) Zhu, H.; Wang, X. L.; Li, Y. L.; Wang, Z. J.; Yang, F.; Yang, X. R. Microwave Synthesis of Fluorescent Carbon Nanoparticles with Electrochemiluminescence Properties. *Chem. Commun.* **2009**, *34*, 5118−5120.
(45) Liu, R. L.; Wu, D. Q.; Liu, S. H.; Koynov, K.; Knoll, W.; Li, Q. An Aqueous Route to Multicolor Photoluminescent Carbon Dots Using Silica Spheres as Carriers. *Angew. Chem., Int. Ed.* **2009**, *48*, 4598−4601.
(46) Zhu, S. J.; Meng, Q. N.; Wang, L.; Zhang, J. H.; Song, Y. B.; Jin, H.; Zhang, K.; Sun, H. C.; Wang, H. Y.; Yang, B. Highly Photoluminescent Carbon Dots for Multicolor Pattering, Sensors, and Bioimaging. *Angew. Chem.* **2013**, *125*, 4045−4049.
(47) Liang, Z. C.; Zeng, L.; Cao, X. D.; Wang, Q.; Wang, X. H.; Sun, R. C. Sustainable Carbon Quantum Dots from Forestry and Agricultural Biomass with Amplified Photoluminescence by Simple NH_4OH Passivation. *J. Mater. Chem. C* **2014**, *2*, 9760−9766.
(48) Hu, Q.; Paau, M. C.; Zhang, Y.; Chan, W.; Gong, X. J.; Zhang, L.; Choi, M. M. F. Capillary Electrophoretic Study of Amine/Carboxylic Acid-Functionalized Carbon Nanodots. *J. Chromatogr. A* **2013**, *1304*, 234−240.
(49) Hao, Y. L.; Gan, Z. X.; Zhu, X. B.; Li, T. H.; Wu, X. L.; Chu, P. K. Emission from Trions in Carbon Quantum Dots. *J. Phys. Chem. C* **2015**, *119*, 2956−2962.
(50) Zheng, C.; An, X. Q.; Gong, J. Novel pH Sensitive N-doped Carbon Dots with both Long Fluorescence Lifetime and High Quantum Yield. *RSC Adv.* **2015**, *5*, 32319−32322.
(51) Zhu, J.; Bian, X. J.; Kong, J. L.; Yang, P. Y.; Liu, B. H. pH-Controlled Delivery of Doxorubicin to Cancer Cells, Based on Small Mesoporous Carbon Nanospheres. *Small* **2012**, *8*, 2715−2720.
(52) Chen, S.; Hai, X.; Xia, C.; Chen, X. W.; Wang, J. H. Preparation of Excitation-Independent Photoluminescent Graphene Quantum Dots with Visible-Light Excitation/Emission for Cell Imaging. *Chem. - Eur. J.* **2013**, *19*, 15918−15923.

DOI: 10.1021/acsami.5b04172
ACS Appl. Mater. Interfaces 2015, 7, 16609−16616